R-09-13

Literature survey: Relations between stress change, deformation and transmissivity for fractures and deformation zones based on *in situ* investigations

Åsa Fransson, Chalmers tekniska högskola

February 2009

Svensk Kärnbränslehantering AB
Swedish Nuclear Fuel
and Waste Management Co

Box 250, SE-101 24 Stockholm
Phone +46 8 459 84 00

ISSN 1402-3091
SKB Rapport R-09-13

Literature survey: Relations between stress change, deformation and transmissivity for fractures and deformation zones based on *in situ* investigations

Åsa Fransson, Chalmers tekniska högskola

February 2009

A pdf version of this document can be downloaded from www.skb.se.

Summary

This literature survey is focused upon relations between stress change, deformation and transmissivity for fractures and deformation zones and aims at compiling and commenting on relevant information and references with focus on data from *in situ* investigations. Main issues to investigate are:

- Impact of normal stress change and deformation on transmissivity, for fractures and deformation zones.
- Impact of shear stress and displacement on transmissivity, for fractures and deformation zones for different normal load conditions.

Considering the line of research within the area, the following steps in the development can be identified. During the 1970´s and 1980´s, the fundamentals of rock joint deformation were investigated and identification and description of mechanisms were made in the laboratory /Bandis et al. 1983, Barton et al. 1985, Evans et al. 1992, Goodman 1974, Witherspoon et al. 1980/. In the 1990´s, coupling of stress-flow properties of rock joints were made using hydraulic testing to identify and describe the mechanisms in the field. Both individual fractures and deformation zones were of interest /Rutqvist 1995, Alm 1999, Martin et al. 1990, Talbot and Sirat 2001/. *In situ* investigations have also been the topic of interest the last ten years. Further identification and description of mechanisms in the field have been made including investigation and description of system of fractures, different types of fractures (interlocked/mated or mismatched/unmated) and how this is coupled to the hydromechanical behavior /Cappa et al. 2006, Guglielmi et al. 2008b, Zangerl et al. 2008/.

In this report, data from *in situ* investigations are compiled and the parameters considered to be important to link fracture deformation and transmissivity are normal stiffness, k_n and hydraulic aperture, b_h. All data except for those from one site originate from investigations performed in granitic rock. Normal stiffness, k_n, and hydraulic aperture, b_h, are correlated, even though data are scattered. In general, the largest variation is seen for small hydraulic apertures and high normal stiffness. The increasing number of contact points (areas) and fracture filling are likely explanations.

To conclude, impact of normal stress change and deformation on transmissivity could be described based on data from *in situ* investigations. The results shown in this compilation present a possibility to estimate normal stiffness, k_n and hydraulic aperture, b_h based on storage coefficient, S, and transmissivity, T, from hydraulic interference tests performed in the area of interest. Concerning the impact of shear stress and displacement on transmissivity, no detailed field data was found. This is in line with the comment by /Guglielmi et al. 2008b/ where the authors express an urgent need to develop *in situ* measurements of both normal and shear displacements. An important future issue is therefore better descriptions of the dependency between shear displacement and transmissivity in the field. Further research within the area of hydromechanical coupling where geology, hydrogeology and geomechanics meet is likely to increase the understanding of all these areas.

Sammanfattning

Denna litteraturstudie behandlar relationen mellan ändring i bergsspänning, deformation och transmissivitet för sprickor och zoner. Syftet är att sammanställa och kommentera relevant information och referenser med fokus på data från undersökningar *in situ*. Det som huvudsakligen behandlas är:

- Inverkan av normalspänningsändring och deformation på transmissiviteten för sprickor och zoner.
- Inverkan av skjuvspänning och förskjutning på transmissiviteten för sprickor och zoner vid olika normalspänningar.

Angående forskningens utveckling inom området kan följande steg identifieras. Under 1970- och 1980-talen undersökte, identifierade och beskrev man grundläggande samband för deformation av sprickor i berg. Detta utfördes främst som laboratoriearbete /Bandis et al. 1983, Barton et al. 1985, Evans et al. 1992, Goodman 1974, Witherspoon et al. 1980/. Under 1990-talet, kopplades spännings- och flödesegenskaper för sprickor i berg med hjälp av hydrauliska fält tester. Detta innebar att man identifierade och beskrev mekanismerna även i fält. Både enskilda sprickor och zoner undersöktes /Rutqvist 1995, Alm 1999, Martin et al. 1990, Talbot and Sirat 2001/. Även de senaste tio åren har undersökningar *in situ* varit av intresse. Ytterligare identifikation och beskrivning av mekanismer i fält har gjorts inklusive undersökning och beskrivning av system av sprickor, olika typer av sprickgeometri (t.ex. matchade, ej matchade sprickor) och hur detta är kopplat till det hydromekaniska beteendet /Cappa et al. 2006, Guglielmi et al. 2008b, Zangerl et al. 2008/.

I denna rapport sammanställs data från undersökningar *in situ* och de parametrar som betraktats som centrala för att koppla deformation och transmissivitet är sprickans normalstyvhet, k_n och dess hydrauliska vidd, b_h. Data från samtliga undersökta platser förutom en kommer från undersökningar utförda i berg med granitisk sammansättning. Sprickans normalstyvhet, k_n och den hydrauliska vidden, b_h, är korrelerade även om data har viss spridning. Generellt ses den största spridningen för de sprickor som har liten vidd och stor normalstyvhet. Det ökande antalet kontaktpunkter (ytor) och sprickfyllnad är troliga förklaringar.

Som slutsats kan sagas att inverkan av normalspänningsändring och deformation på transmissiviteten (för sprickor och zoner) kan beskrivas baserat på data från undersökningar *in situ*. Sammanställningen pekar på en möjlighet att skatta normalstyvheten, k_n och den hydrauliska vidden, b_h med hjälp av magasinskoefficienten, S, and transmissiviten, T, från interferenstester utförda i det specifika området. Beträffande inverkan av skjuvspänning och förskjutning på transmissiviteten hittades inga detaljerade fältdata. Detta är i linje med /Guglielmi et al. 2008b/ som uttrycker ett akut behov för att utveckla metoder för mätningar *in situ* för både normal- och skjuvdeformation. En viktig framtida fråga är därför en bättre beskrivning av kopplingen mellan skjuvdeformation och transmissivitet i fält. Fortsatt forskning inom det hydromekaniska området som kopplar geologi, hydrogeologi och geomekanik kommer sannolikt att öka förståelsen för samtliga områden.

Contents

1 Introduction

1.1 Background

For a nuclear waste repository, mechanical and thermo-mechanical processes in the geosphere are important to both performance and long-term safety. Examples of possible consequences are direct mechanical damage but changes of the mechanical conditions may also result in changes of the hydraulic properties of the rock mass.

This report reviews some of the recent literature on relations between deformation and transmissivity for fractures and deformation zones. Its main focus is on experiences from field experiments.

1.2 Objectives and scope

The literature survey is focused upon relations between stress change, deformation and transmissivity for fractures and deformation zones and aims at compiling and commenting on relevant information and references with focus on data from *in situ* investigations.

Main issues are:

- Impact of normal stress change and deformation on transmissivity, for fractures and deformation zones.
- Impact of shear stress and displacement on transmissivity, for fractures and deformation zones for different normal load conditions.

2 Models describing relations between stress change, deformation and transmissivity

This section aims at briefly presenting some models describing the relations between stress change, deformation and transmissivity. Main focus is on the behaviour of individual fractures. The following is included:

- Normal stress change, deformation and transmissivty.
- Storage coefficient, normal stiffness and transmissivity.
- Shear stress, displacement and transmissivity.

The descriptions are kept short as a general orientation and other compilations of models for estimating fracture mechanical and hydromechanical response are found in e.g. /Rutqvist and Stephansson 2003/ and /Alm 1999/.

As a basis and link to the papers reviewed in this report, the terminology used by the Swedish Nuclear Fuel and Waste Management Co (SKB) in their geological site descriptive model (geology: /Munier et al. 2003/; rock mechanics: /Andersson et al. 2002/; hydrogeology: /Rhén et al. 2003/) is presented. According to /Munier et al. 2003 and Rhén et al. 2003/, a deformation zone is a two-dimensional structure in which deformation has been concentrated (or is concentrated for active faults). The zone can be brittle, ductile or both (composite). The term fracture zone can be used for a brittle deformation zone or the brittle part of a composite deformation zone. In the site descriptive models only fracture zones larger than 1 km are described explicitly, e.g. /Andersson et al. 2002/. The remaining zones are described statistically within separate rock units.

2.1 Stress change and deformation: general

The deformation of fractures and deformation zones and changes of the hydraulic conditions depends upon the situation of stress. This will change due to e.g. phase, depth and proximity to the tunnel. For SKB, the phases can be divided into the construction and operational phases, the initial temperate period and a subsequent glacial cycle, see e.g. /Hökmark et al. 2006/.

Considering the situation of stress, the effective normal stress is defined as:

$$\sigma'_n = \sigma_n - p \tag{2-1}$$

and the fracture normal deformation may be expressed:

$$\Delta u_n = \frac{\Delta \sigma'_n}{k_n} \tag{2-2}$$

In these expressions, σ_n is the total normal stress, p is the fluid pressure and k_n is the fracture normal stiffness. Figure 2-1 shows three drawings from /Gothäll 2009/ representing the change in geometry for an unmated fracture with increasing load (from a–c). The lower stiffness of an unmated or mismatched joint (Figure 2-1) compared to an interlocked is the expected result of stress concentration over a lower actual contact area. The resulting system of channels, Figure 2-1c, would explain the observed flow of water and the residual transmissivity under extremely high normal stress.

The rate of deformation is greatest at low values of normal stress, see Figure 2-2a. This has been described by e.g. /Goodman 1974, Bandis et al. 1983, Evans et al. 1992/. Important to have in mind is that fractures have different characteristics depending on the fracture formation resulting in different type or extent of mineral coating or filling, this can have a major impact on the fracture stiffness and the permeability /Gale 1990/.

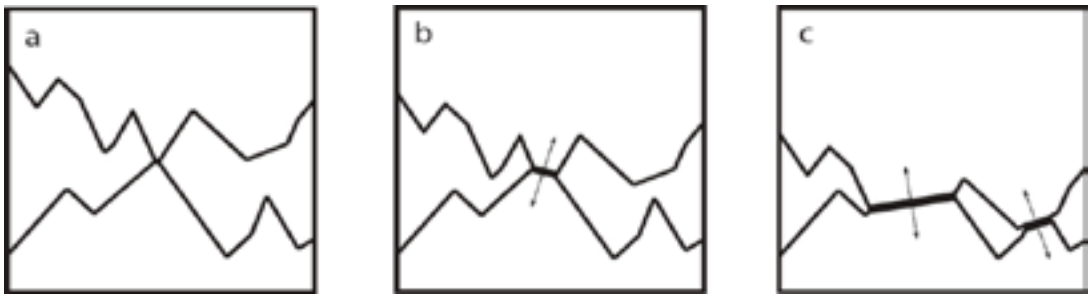

Figure 2-1. *a) The two random, unmated surfaces (example of a mismatched joint) are brought into contact with a minimum normal load. b) The load has increased and the rock is being crushed. c) The load is increased again and the deformation of rock increases and additional points of contact are formed. From /Gothäll 2009/.*

Both normal and shear stresses influence the deformation and /Guglielmi et al. 2008b/ describe the situation for a fracture where the opposing joint walls are pressed together under a positive effective normal stress. In addition, the shear stress acts parallel to the fracture plane and perpendicular to the effective normal stress that resists a sliding motion. Reducing the effective normal stress leads to a normal opening and reduced shear strength. During fracture shear movements the aperture will change due to dilation. In this case the asperities can be sheared through or overridden.

2.2 Normal stress change, deformation and transmissivity

2.2.1 Goodman model

The model (hyperbolic) presented by /Goodman 1974/ can be expressed:

$$\frac{\sigma'_n - \sigma'_{ni}}{\sigma'_{ni}} = \frac{\Delta u}{V_{mi} - \Delta u} \tag{2-3}$$

Here, V_{mi} is the maximum possible closure at the initial reference stress, σ'_{ni}. Further, the initial normal stiffness is estimated:

$$k_{ni} = \frac{\sigma'_{ni}}{V_{mi}} \tag{2-4}$$

Based on the above, Equation 2-3 could also be written:

$$\Delta u_n = \frac{\sigma'_{ni}}{k_{ni}}\left(1 - \frac{\sigma'_{ni}}{\sigma'_n}\right) \tag{2-5}$$

where Δu_n is the fracture normal deformation and σ'_{ni} and k_{ni} are respectively the total normal stress and the fracture normal stiffness at an initial reference stage /Rutqvist 1995/, see Figure 2-2a. Going from a mechanical to a hydromechanical response, Goodman´s equation could be reformulated to give a transmissivity:

$$T = T_i + \Delta T = \frac{\rho_w g}{12\mu_w}\left(e_i + \Delta e\right)^3 = \frac{\rho_w g}{12\mu_w}\left(e_i + f\Delta u_n\right)^3 = \frac{\rho_w g b_h^3}{12\mu_w} \tag{2-6}$$

The equation for estimate of transmissivity is also referred to as the cubic law, see e.g. /Witherspoon et al. 1980/ and /Gale 1990/. Equation 2-6 includes the hydraulic aperture, b_h, commonly used in this report. Here, e_i is the initial hydraulic aperture at the initial reference stress, σ'_{ni}. The change in

hydraulic aperture, Δe, compared to the mechanical normal displacement, Δu_n is obtained using a factor, f, see Equation 2-6, compensating for the deviation of flow in a natural rough fracture from the ideal case of parallel smooth fracture surfaces. The density and viscosity of the fluid, ρ_w and μ_w, and the acceleration due to gravity, g, are also included in the equation. The validity of the cubic law for fluid flow in a deformable fracture has been investigated by /Witherspoon et al. 1980/. In /Rutqvist et al. 1998/, the hydraulic normal stiffness, κ_n, is used where

$$\kappa_n = \frac{k_n}{f} . \tag{2-7}$$

The hydraulic stiffness is equal to or higher than the mechanical stiffness since the factor f is equal to or less than 1 /Rutqvist 1995/.

The relation between mechanical mean aperture and hydraulic aperture varies which is exemplified in e.g. /Hakami 1995/ and /Olsson and Barton 2001/ presenting comparisons of mechanical apertures with theoretical smooth wall conducting apertures. According to /Hakami 1995/ the ratio between mechanical mean aperture and hydraulic aperture was 1.1–1.7 for a mean aperture of 100–500 µm. This would result in a value of the factor f of 0.6 to 0.9, see /Rutqvist et al. 1998/. In /Olsson and Barton 2001/ experimental data show that for smooth walls or very wide apertures the mechanical apertures and theoretical smooth wall conducting apertures are equal.

2.2.2 Bandis and Barton model

Another model (hyperbolic) to describe the normal deformation is found in /Bandis et al. 1983/ and /Barton et al. 1985/:

$$\delta = \frac{\sigma_n'}{k_{n0} + \sigma_n'/\delta_{\max}} \tag{2-8}$$

The equation includes the current normal closure, δ, the maximum normal closure, δ_{max}, and the normal stiffness at the zero stress intercept, k_{n0}, see Figure 2-2a. In /Guglielmi et al. 2008b/ an empirical hyperbolic relationship is suggested:

$$k_n = \frac{1}{a\left(1 - \frac{b}{a} b_h\right)^2} = \frac{k_{n\max}}{\left(1 - \frac{b_h}{b_{h\min}}\right)^2} \tag{2-9}$$

where a and b are empirical parameters and b_h is the hydraulic aperture.

2.2.3 Evans model

This (logarithmic) model is described in e.g. /Evans et al. 1992, Kohl et al. 1995, Zangerl et al. 2008/ and includes a parameter referred to as the stiffness characteristic, $dk_n/d\sigma_n'$, that is evaluated from a stress-deformation plot. In this case, the change in mechanical aperture resulting from a change in stress from a reference value, σ'_{n0}, can be described:

$$-\Delta u_n = \left(dk_n/d\sigma_n'\right)^{-1} \ln \frac{\sigma_n'}{\sigma_{n0}'} \tag{2-10}$$

By multiplying the value of $dk_n/d\sigma'_n$ to any effective normal stress level, σ'_n, the normal stiffness of the fracture, k_n, can be obtained:

$$k_n = \left(dk_n/d\sigma_n'\right) \cdot \sigma_n' \tag{2-11}$$

where the stiffness is zero at zero normal stress.

2.3 Storage coefficient, normal stiffness and transmissivity

According to e.g. /Doe and Geier 1990/ a storativity (storage coefficient) of a fracture can be expressed:

$$S = \rho_f g\left(\frac{1}{k_n} + eC_f\right) \tag{2-12}$$

where e is the fracture (void) aperture and C_f the fluid compressibility. Considering single fractures the authors comment that due to the very small fluid volumes the stiffness component may be dominant resulting in:

$$S = \rho_f g\left(\frac{1}{k_n}\right) \tag{2-13}$$

In /Rhén et al. 2008/ an expression, found by regression analysis, describes the relationship between transmissivity, T, and the storage coefficient, S, see Section 3.2.2.

2.4 Shear stress, displacement and transmissivity

/Olsson and Barton 2001, Olsson 1998, Rutqvist and Stephansson 2003/ describe the relation between shear displacement and transmissivity. The dilation curve relating Δu_n and Δu_s see Figure 2-2c can be calculated using the expression:

$$\Delta u_n = \Delta u_s \tan d_{mob} \tag{2-14}$$

where the mobilized dilation angle, d_{mob}, is:

$$d_{mob} = \frac{1}{M} JRC_{mob} \log_{10}\left(JCS/\sigma_n\right) \tag{2-15}$$

The parameter M, is referred to as a damage coefficient that is given values of 1 or 2 for shearing under low or high normal stress respectively. JRC_{mob} is the mobilized joint roughness coefficient, and JCS the joint compressive strength. Further, the resulting mechanical aperture is calculated:

$$E = E_0 + \Delta u_n = E_0 + \Delta u_s \tan\left[\frac{1}{M} JRC_{mob} \log_{10}\left(JCS/\sigma_n\right)\right] \tag{2-16}$$

Finally, to obtain a hydraulic aperture the following two expressions are suggested depending upon the shear displacement:

$$e = \frac{E^2}{JRC_0^{2.5}} \qquad u_s \le 0.75 u_{sp} \tag{2-17}$$

$$e = \sqrt{E} \cdot JRC_{mob} \qquad u_s \ge u_{sp} \tag{2-18}$$

Equation 2-17 describes a pre-peak/peak behavior and Equation 2-18 a post-peak behavior.

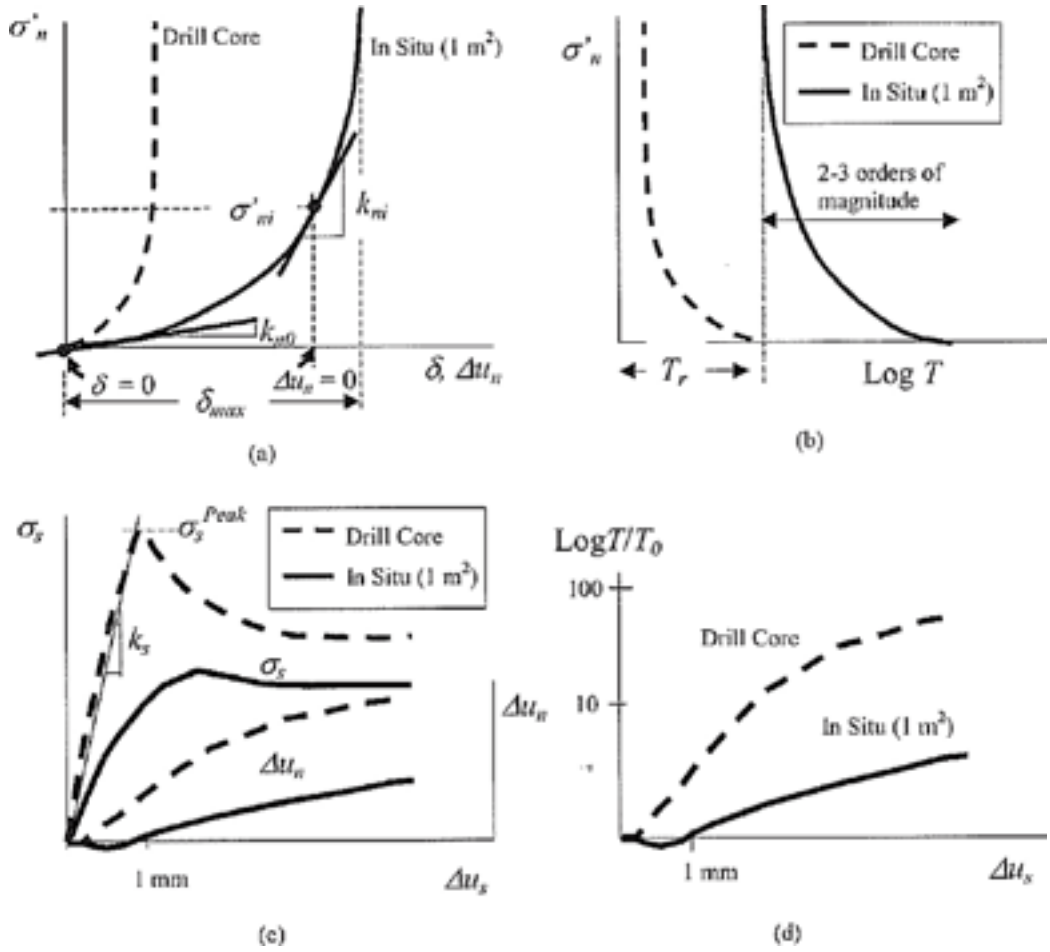

Figure 2-2. *Typical mechanical and hydromechanical fracture responses under normal closure (a, b) and shear (c, d), from /Rutqvist and Stephansson 2003/. Goodman model: Δu_n is fracture normal deformation, σ'_{ni} is the total normal stress and k_{ni}, the fracture normal stiffness at an initial reference stage. Bandis and Barton model: the current normal closure is δ, the maximum normal closure, δ_{max}, and the normal stiffness at the zero stress intercept, k_{n0}. T_r is the residual transmissivity at high compressive stress. Different behaviors are seen for drill core- and in situ investigations.*

2.5 Comments

According to /Rutqvist and Stephansson 2003/ the method presented in /Bandis et al. 1983/ is the most commonly applied followed by the one presented in /Evans et al. 1992/. /Rutqvist and Stephansson 2003/ also comment that the Bandis model, in general, has shown to match mated fractures better and the Evans model is better for unmated fractures. The hydromechanical response in Figure 2-2b includes the residual transmissivity, T_r. /Rutqvist and Tsang 2008/ comment that this is an important parameter at high normal stress.

3 Data from *in situ* investigations

This section mainly compiles results from *in situ* experiments investigating both fractures and deformation zones. Figure 3-1 presents the references that include detailed field data and shows the approximate depth (or depth interval) where the field experiments were performed. The parallel, inclined lines in Figure 3-1, represent deformation zones and data originate from /Martin et al. 1990/ and /Rhén et al. 2008/. Information concerning the field experiments is presented in Table 3-1. Data from field experiments investigating individual fractures (fractured rock) are found in /Rutqvist et al. 1998, Alm 1999, Cappa et al. 2006, Guglielmi et al. 2008b/.

3.1 Fractures

3.1.1 Rock Mechanics Laboratory, Luleå and Äspö Hard Rock Laboratory

/Rutqvist et al. 1998/ investigate the determination of fracture storativity in hard rocks using high-pressure injection testing. The results verify that the storage is related to the fracture opening. Both the stiffness of the fracture and the ambient rock mass are of importance but in most practical cases the storage is controlled by the stiffness of the fracture. Fractures in granitic rocks at two sites, the Rock Mechanics Laboratory of Luleå University of Technology (RML, Luleå) and the Äspö Hard Rock Laboratory (Äspö HRL), are tested. The depths of fractures are between 80 to 420 meters and the equipment consisted of a double packer with a 0.65 packer separation. For Luleå, fractures are widely spaced and tests are therefore considered to be on single subhorizontal fractures and for Äspö, few open fractures dominated the inflow even though they were part of the most conductive zones intersecting the tested borehole (KLX02). Two-pressure injection tests and multiple-pressure

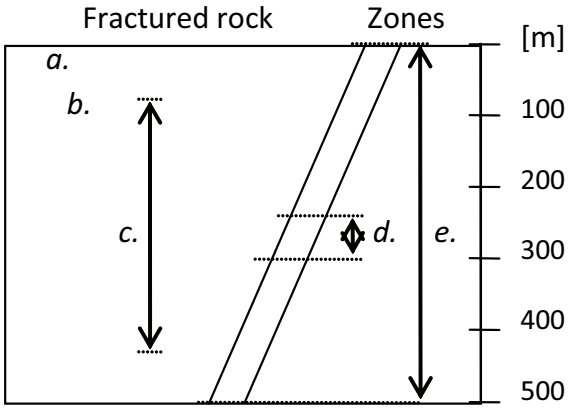

a) Coaraze Laboratory site: /Cappa et al. 2006, Guglielmi et al. 2008ab/.

b) Röda sten Rock Laboratory (RL): /Alm 1999/.

c) Rock Mechanics Laboratory (RML), Luleå and Äspö Hard Rock Laboratory (HRL): /Rutqvist 1995, Rutqvist et al. 1998/.

d) Underground Research Laboratory (URL), Canada: /Martin et al. 1990/.

e) Äspö Hard Rock Laboratory (HRL) and Laxemar: /Rhén et al. 2008/.

Figure 3-1. *Compilation of field experiments. Letters (a–d) indicate field experiments and depth (or depth interval) where investigations were performed. Field experiments (a–c) investigated individual fractures and (d–e) deformation zones, see details in Table 3-1.*

Table 3-1. Compilation of field experiments.

Test site Reference	Rock, Fracture type	Depth [m]	Effective normal stress [MPa]	(Equivalent) hydraulic aperture [µm] Transmissivity [m^2/s]	(Hydraulic) normal stiffness [GPa/m]
a. Coaraze Laboratory, France /Cappa et al. 2006/ /Guglielmi et al. 2008a/ /Guglielmi et al. 2008b/	Carbonate rock Individual fractures, Fracture system	Surface, 30 m × 30 m × 15 m	σ_n:0.1–0.5 dP: 0.08	10, 50, 100 µm (I) /Cappa et al. 2006/ 33–530 µm (II) from figure, /Guglielmi et al. 2008b/ – –	100, 50, 17 1.4–200
b. Röda Sten Rock Laboratory, Göteborg /Alm 1999/	Granite Individual fracture	70 (11 meter below tunnel floor)	0.4–1.2	200–400 µm $1{\cdot}10^{-5}$– $5{\cdot}10^{-5}$ m^2/s (approx. values from tables)	2–4
c. Rock Mechanics Laboratory of *Luleå* University of Technology /Rutqvist et al. 1998/	Granitic Single subhorizontal fractures	81–417	1.4–7.3	8–22 µm $4.3{\cdot}10^{-10}$– $4.1{\cdot}10^{-8}$ m^2/s	30–1,100
c. *Äspö* Hard Rock Laboratory /Rutqvist et al. 1998, Rutqvist 1995/	Granitic Few open fractures part of zones intersect. KLX02	266–338	3.9–4.8	19–164 µm $5.7{\cdot}10^{-9}$– $3.7{\cdot}10^{-6}$ m^2/s	75–1,000
d. Underground Research Laboratory (URL), Canada /Martin et al. 1990/	Granite Shear zone and joints	240–300	0.5–20 (mean)	21–416 µm –	3.2–494 (mean)
e. Äspö Hard Rock Laboratory and Laxemar: /Rhén et al. 2008/	Granitic, Deform. zones	0–500	–	70–800 µm $\approx 1{\cdot}10^{-7}$–$1{\cdot}10^{-3}$ m^2/s (LogT: –6.5 to –3.5)	See expression Section 3.2.2.
Compilation of in situ experiments /Zangerl et al. 2008/	Granitic rock	Varies	0.07–10	No transmissivity or hydraulic aperture data.	0.4–1,100

injection tests were performed. Analyses were made using coupled hydromechanical finite element simulations (ROCMAS). The model of the fracture is axisymmetric with a circular-shaped rock fracture intersecting a borehole. Mineral filled or coated fractures, with low stiffness would have the largest storativity. The lowest effective stress for the tests (Äspö HRL) was 1.4 MPa and the hydraulic stiffness varied between 30–1,100 GPa/m for apertures ranging from 8 to 164 µm, see /Rutqvist et al. 1998, p. 2558/ and Table 3-1 and Figure 3-1. The hydraulic stiffness for the largest apertures (164 µm and 60 µm) are uncertain (<1,000 GPa/m). Data from Äspö HRL are also discussed in /Rutqvist 1995/. The relation between hydraulic stiffness and normal stiffness is presented in Section 2.2.1. In /Rutqvist et al. 1998/ the factor *f* relating the two parameters was set to 0.3.

3.1.2 Röda sten Rock Laboratory, Göteborg

/Alm 1999/ describes the hydromechanical behavior of a pressurized single fracture, and a central part of the work is an *in situ* experiment. The test site, Röda Sten Rock Laboratory, is located in Göteborg at 70 meters depth. The rock is a massive granite and the investigated fracture is found 11 meters beneath the tunnel floor. Seven vertical boreholes were drilled within the fracture and an area of 16 m^2. An estimate of the normal stress across the fracture was about 2 MPa. According to the stress function (Kirsch equations) presented in /Hoek and Brown 1982/, the fracture should be unaffected by secondary stresses resulting from the tunnel. /Alm 1999/ comment that due to the complex geometry of tunnels and caverns, the stress situation is somewhat uncertain. For the investigations, double packers with a 0.5 meter packer separation were used. During the test, the whole fracture was pressurized at five different pressure steps, all below the normal stress to avoid

hydraulic jacking. Predictions were made based on /Evans et al. 1992/ and following the tests, the transmissivity distribution within the fracture was evaluated from slug tests in all boreholes for the different pressure steps. For the pressure step 0.8 to 1.0 MPa, the change in hydraulic aperture was 52.3 μm and for the pressure step 1.4 to 1.6 MPa, the change was 120 μm. Dividing the pressure step by the change in hydraulic aperture gives an estimate of the stiffness of 3.8 (≈ 4) and 1.7 (≈ 2) MPa/mm (or GPa/m), see /Alm 1999, p. 84/. Hydraulic apertures varies within the fracture but for the lowest injection pressure (0.8 MPa) it is approximated to 200 μm and for the highest injection pressure 400 μm, see /Alm 1999, p. 76 and 82/. When changing the effective stress by 0.8 MPa (from 1.2 to 0.4 MPa) the overall transmissivity of the fracture was increased by a factor of 20. The difference between the highest and the lowest transmissivity within the fracture was a factor of 10, this relationship was retained during the pressurization. Analyses of the deformations show that stiffness characteristics within this same fracture vary between 3.0 and 6.8 mm^{-1}. Data indicate that the smaller the hydraulic aperture, the stiffer the fracture becomes.

3.1.3 Coaraze Laboratory site, France

Results from the Coaraze Laboratory site in France have been presented in e.g. /Cappa et al. 2006, Guglielmi et al. 2008a, Guglielmi et al. 2008b/. In these papers comments on both individual fractures and the fracture system are given. The geometry of individual fractures in terms of fractures being interlocked or mismatched is of importance.

/Guglielmi et al. 2008b/ present a new *in situ* approach for hydromechanical characterisation of fractures. Fast (seconds) pressure pulse tests are performed for isolated sections of a borehole and both deformation ($\pm 10^{-7}$ m) and fluid pressure (±1 kPa) for intersected fractures are measured. The method is referred to as the High-Pulse Poroelasticity Protocol (HPPP) using a probe with fiber-optic sensors that allows high-frequency measurements. In this case, the tests were performed at the Coaraze site, France. The site consists of carbonate rock (30 m × 30 m × 15 m) and is an unconfined aquifer drained by a natural spring. The rock is cut by 12 bedding planes and two sets of approximately orthogonal, near vertical faults. To investigate local fracture properties, nine corings were performed. Tests were performed with a pressure (10 to 120 kPa) that was lower than the ambient state of stress on the fracture to prevent hydraulic fracturing. Field measurements and coupled hydromechanical numerical models are used to estimate the stiffness and hydraulic aperture of fractures. Considering the behaviour of more than one fracture, the authors comment that for parallel fractures, the poroelastic opening of the tested fracture induces a poroelastic closing of surrounding parallel fractures. If the network geometry and the state of stress are known close to the test, hydromechanical properties of the tested fracture as well as of adjacent fractures (normal or shear) can be estimated. Nine HPPP tests were performed and the normal stiffness values are between 1.4 GPa/m and 200 GPa/m. The hydraulic apertures varied from 33 μm to 530 μm. The average normal stiffness for faults was 19 GPa/m and for bedding planes 115 GPa/m. The corresponding hydraulic apertures were 280 μm for the faults and 60 μm for the bedding planes. A graph presenting a comparison of fracture properties (hydraulic aperture and normal stiffness) estimated based on *in situ* tests (HPPP-tests) and laboratory tests show good agreement. According to a figure presented in the paper, the in situ tests were performed with a normal stress, σ_n, between 1 to $5 \cdot 10^5$ Pa and a δP of 80 kPa. For the laboratory tests the normal stress, σ_n, was 2 to $6 \cdot 10^7$ Pa and δP 1 to $4 \cdot 10^6$ Pa. Results referred to as Coaraze I included in Figure 4-1 and Figure 4-2 are from earlier studies at the site /Cappa et al. 2006, p. 1073/. For these data, the two faults had the largest apertures (100 and 50 μm) and the bedding planes the smallest (10 μm), see Table 3-1. Coaraze II includes approximate values taken from a figure in /Guglielmi et al. 2008b, Figure 5/.

3.1.4 Compilation of in situ experiments /Zangerl et al. 2008/

/Zangerl et al. 2008, p. 1503–1504/ present a compilation of normal stiffness of fractures in granitic rock from laboratory tests and *in situ* experiments. The compilation is based on the semi-logarithmic closure law presented in Section 2.2.3 described as the Evans model where $dk_n/d\sigma'_n$ is referred to as the "stiffness characteristic". By multiplying the value to any effective normal stress level, σ'_n, Equation 2-11, the normal stiffness of the fracture, k_n, can be obtained. /Zangerl et al. 2008/ compiles the range of effective normal stress, $\sigma'_{n\,min}$ to $\sigma'_{n\,max}$, and the stiffness characteristics based on seven different references including the data from Luleå and Äspö in /Rutqvist et al.1998/ and a

joint investigated by /Martin et al. 1990/, see below. The stiffness characteristics and the effective normal stress range, $\sigma'_{n\,min}$ to $\sigma'_{n\,max}$, are used to estimate a corresponding interval of normal stiffness from k_{nmax} to k_{nmin}, see Figure 4-3. For three of the references including the data presented in /Rutqvist et al. 1998/ and /Martin et al. 1990/ only $\sigma'_{n\,max}$ is available. According to these references (Sections 3.1.1 and 3.2.1), /Rutqvist et al. 1998/ describe *hydraulic normal stiffness* and /Martin et al. 1990/ the *normal stiffness*. However, the compilation of /Zangerl et al. 2008/ do not consider this, data are treated in the same way referring to fracture normal stiffness.

3.2 Deformation zones

3.2.1 Underground Research Laboratory (URL), Canada

/Martin et al. 1990/ describe the characterization of normal stiffness and hydraulic conductivity of a major shear zone and associated joints in granite. The Underground Research Laboratory (URL) is situated in the Lac du Bonnet granite batholiths in Canada. The fracture zones investigated are found at a depth of approximately 240–300 meters and have chloritic slip surfaces, and cataclastic zones. The latter contain breccias and clay-gouge and have a thickness between 20 mm and 1 meter. The *in situ* stress was determined using several different techniques (overcoring, hydraulic fracturing, back-analysis of excavation response, microseismic observations etc). For the hydrogeological description, both short-duration permeability tests and long duration tests were performed. The areas of lowest normal stress were found to have the highest permeability and areas of highest normal stress had the lowest permeability. For monitoring of the coupled hydromechanical response of joints intersecting the boreholes a special instrumentation was developed. Boreholes were tested in sections and a significant decrease in normal stiffness was found when the measurements approached the cataclastic zone. According to the authors, the normal stiffness of the cataclastic zone seems to be stress independent. The mean effective normal stress varies between 0.5 and 20 MPa, see /Martin et al. 1990, p. 554/. The *in situ* normal stiffness (mean) was between 3.2 and 494 GPa/m and the equivalent single fracture hydraulic aperture (estimated for each test interval) had values ranging from 21 to 416 µm. Data are included in Figure 4-1, Figure 4-2 and Figure 4-3 (part of evaluation made by /Zangerl et al. 2008/. In Figures 4-1 and 4-2, data originating from the zone (Fracture zone) are identified by a plus-sign and data for a series of subparallel joints forming a fracture zone (Joint) are identified by a minus-sign. For one of the tested boreholes, several sections were investigated and the normal stiffness for the sections has a range of 4.4 to 170 GPa/m The estimated equivalent single fracture hydraulic aperture for the full section would be 280 µm and this value and the median stiffness (identified by an unfilled triangle) are included in Figure 4-1 and Figure 4-2.

3.2.2 Äspö Hard Rock Laboratory and Laxemar

/Rhén et al. 2008/ describe an expression for the storage coefficient, *S*, as a function of transmissivity, *T*, in deformation zones for data originating from hydraulic interference tests at the Äspö Hard Rock Laboratory and the Laxemar area next to Äspö:

$$S = 0.0109 \cdot T^{0.71} \qquad (3\text{-}1)$$

The correlation coefficient, r^2, for the data was found to be 0.62. The compilation is made for an approximate transmissivity interval of –6.5 to –3.5 (logT) m^2/s and for a depth down to 500 m. Data are the result from several years of investigations of the Äspö – Laxemar area. For the interference tests, pumping is performed in one borehole and the observation is made in another borehole. Estimates of the storage coefficient were based on the following /Rhén et al. 2008/: The observation section should be fairly close to the pumped section in a deformation zone (within 300 m); the observation section data used was assumed to be well-connected to the deformation zone studied and; no other major hydraulic feature was expected to interfere so that a radial flow assumption for one feature could be valid. Further, observation sections with low and/or slow responses were excluded for well defined deformation zones. Tests with what seemed to be a complex geometry of zones were also excluded. For remaining observation sections, the geometric mean of *S* was plotted against the transmissivity of the pumped borehole section.

Equations 2-13 and 3-1 give an expression describing a relationship between the transmissivity, normal stiffness and the storage coefficient for the data:

$$S = \rho_f g\left(\frac{1}{k_n}\right) = 0.0109 \cdot T^{0.71} \tag{3-2}$$

resulting in:

$$k_n = \rho_f g\left(\frac{1}{0.0109 \cdot \left(\frac{\rho_f g b_h^{\,3}}{12\mu}\right)^{0.71}}\right) \tag{3-3}$$

The relationship is included in Figures 4-1 and 4-2 (Äspö HRL & Laxemar). Values of the storage coefficient, *S*, are within a factor of ten larger or ten smaller than the relationship presented in Equation 3-1. This is shown as 10**S* and 0.1**S* in Figures 4-1 and 4-2.

3.2.3 Other examples: *in situ* and laboratory data

References below are not included in the compilation of data in Figure 4-1 to 4-3 and some tests are performed in the laboratory.

/Chester and Logan 1986/ look at mechanical properties of brittle faults based on observations from the *Punchbowl Fault Zone* in California (part of the San Andreas fault). The authors suggest a model with three mechanical units including: the undeformed host rock; a damaged zone; and a gouge layer. Experiments were performed on collected specimens from the fault and the gouge layer had significantly lower permeability, strength and elastic modulus. In addition there was a gradual increase in permeability and a decrease in strength and elastic modulus toward the main gouge zone.

Also in unconsolidated sediments (*Roer Valley Rift System*, Netherlands) the fault core is characterised by reduced hydraulic conductivity /Bense et al. 2003/. That a strongly sheared fault core would hinder fluid flow and mainly allowing large flow through the damaged zone of a fault zone is in agreement with the results in /Zhang et al. 1999/. /Zhang et al. 1999/ comment that the distribution of fluid pressure in natural fault zones could be very heterogeneous. This was concluded based on the evolution of permeability anisotropy and pressure dependency of permeability in experimentally sheared gouge materials.

Also for major strike-slip zones in Southwest Japan (the *Median Tectonic Line, MTL*) the central slip zone gouges have the lowest permeabilities /Wibberley and Shimamoto 2003/. The MTL separate the Ryoke granitic gneisses and mylonites from the Sambagawa schists. The differing lithologies gave rise to a highly asymmetric fault zone structure. Important for the fault zone permeability structure is the interplay between fracture dilatancy, cementation, shear-enhanced compaction and clay formation. Permeability was measured in the laboratory. The authors also comment on permeability data for fault gouge from other investigations from the San Andreas fault, the Carboneras fault and the Nojima fault. At effective pressures of between 50 and 180 MPa the permeability is between 10^{-18} and 10^{-22} m^2.

/Seront et al. 1998/ investigated hydromechanical properties of core samples from the *Stillwater seismogenic normal fault* in Dixie Valley, Nevada. Here as well, three primary units were identified in the fault zone: a relatively wide fault core; a damage zone (with arrays of mesoscopic fractures); and protolith. Hydromechanical properties of representative core samples were characterised in the laboratory. Investigations suggest that fluid flow and changes in fluid storage are concentrated in the damage zone. Further, permeability decreased with increasing effective pressure, decreasing

porosity and connectivity of pore space. The permeability of the damage zone was several orders of magnitude higher than for the protolith and fault core. The authors comment that unless there is massive influx of fluids, it is unlikely that pore pressure excess can be maintained in this highly permeable zone.

/Evans et al. 2005/ describe the effect on permeability creation and damage due to massive fluid injections into a 3.6 km deep borehole with a 750 m long open section at the lower part. The experiment was performed at the *Soultz Hot Dry Rock test site*, France. Before injection, 17 fractures were identified as permeable and following injection the number was at least 95. The creation and enhancement of permeability was limited to the hydrothermally altered sections at the intersection of cataclastic shear zones. Zones where almost all the naturally permeable fractures were located. Major structures with a strongly developed alteration did appear less susceptible to transmissivity enhancement through shear than lesser structures.

4 *In situ* data compilation and discussion

4.1 Impact of normal stress change and deformation on transmissivity

In this section, data originating from investigations of both fractures and deformation zones are compiled. To motivate that this is a reasonable approach, Section 4.2 includes a suggestion of how to estimate equivalent mechanical properties for rock and fractures. The hypothesis is that if individual fractures or deformation zones are subjected to a change in stress, the individual (only) fracture or the (open) fracture with the lowest stiffness within the deformation zone will be of greatest importance for the behavior.

Figure 4-1 (log-log plot) and Figure 4-2 (lin-lin plot) compile data from most of the references presented in Table 3-1. The figures include hydraulic aperture (equivalent) and hydraulic normal stiffness from /Rutqvist et al. 1998, Alm 1999, Cappa et al. 2006, Guglielmi et al. 2008b, Martin et al. 1990, Rhén et al. 2008/.The largest apertures in general have the lowest stiffness and the lowest effective normal stress.

Figure 4-3 presents examples of relations between stiffness and normal stress were an increase in stiffness is related to an increase in effective stress. The figure includes effective normal stress and estimated normal stiffness, from k_{nmin} to k_{nmax}, using: Equation 2-11; the intervals of effective normal stress, $\sigma'_{n\,min}$ and $\sigma'_{n\,max}$ and; the stiffness characteristics from /Zangerl et al. 2008/. The references: (1) /Rutqvist et al. 1998/; (2) /Martin et al. 1990/; (3) /Makurat et al. 1990/; (4) /Jung 1989/; and (5) /Pratt et al. 1977/, are included in /Zangerl et al. 2008/, see Figure 4-3. For data from /Rutqvist et al. 1998/ (RML, Luleå and Äspö HRL) the hydraulic normal stiffness is presented and if multiplying this stiffness by the factor f of 0.3 (see Sections 2.2.1 and 3.1.1), this would not change the general appearance of the figure to any large extent.

Concerning Figures 4-1 and 4-2, the following comments are considered important:

- All data except those from the Coaraze site originate from granitic rock (see Table 3-1). Even though data are scattered, normal stiffness, k_n, and hydraulic aperture, b_h, seem correlated. Data from Äspö HRL and Laxemar /Rhén et al. 2008/ estimated from the storage coefficient, S, and transmissivity; T, from hydraulic interference tests seems to agree as well, thus giving a relationship between the parameters, normal stiffness, k_n, storage coefficient, S, and hydraulic aperture, b_h for the data. This presents a possibility to estimate k_n and b_h based on storage coefficient, S, and transmissivity, T, from hydraulic interference tests for the investigated area. For Äspö HRL and Laxemar data, the relation between k_n and b_h (Equations 3-1 to 3-3) based on 0.1*S and 10*S are also included since the storage coefficient, S, for a certain transmissivity, T, are found within this interval.
- Two main groups of data could be identified, see Figure 4-2:
  a) *Low stiffness – larger variation in aperture (low effective stress due to e.g. shallow depth, orientation, solid line).* /Guglielmi et al. 2008b/ include an example with an aperture of 530 μm and a stiffness of 1.4 GPa/m. The effective stress is low (< 0.5 MPa). A large fracture normal deformation could be expected.
  b) *Small apertures – larger variation in stiffness (larger variation in effective stress due to e.g. larger depth, orientation, dashed line).* /Rutqvist et al. 1998/ include an example with an aperture of 12 μm and a stiffness of 1,100 GPa/m. The effective stress was estimated to 7.3 MPa. A small fracture normal deformation could be expected.

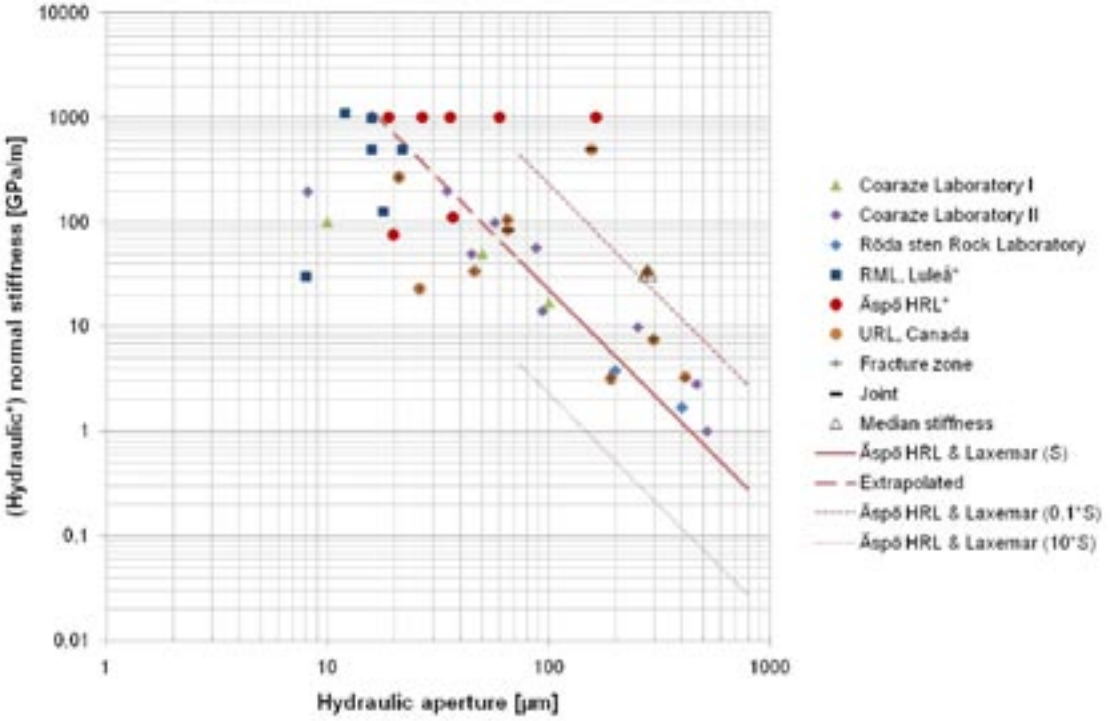

Figure 4-1. *Compilation of (equivalent) hydraulic aperture and normal stiffness (or hydraulic normal stiffness, identified by *). The symbols: +; – and;unfilled triangle are related to URL, Canada data, see section 3.2.1. Coaraze Laboratory I and II originate from the same site but two different papers, see Section 3.1.3.*

In Figure 4-2, simplified sketches based on Figure 2-1a and Figure 2-1c are included. In the lower right hand corner (large aperture – low stiffness), few contact points, low stiffness and large aperture is expected (low effective stress).

In the upper left hand corner (small aperture – high stiffness), many contact points, high stiffness and a small aperture is expected (high effective stress). Intersecting one of the channels is likely to result in an overestimated aperture. That could be the case for e.g. the large aperture – high stiffness data from Äspö HRL (red, filled circles, Figures 4-1 and 4-2).

Variations in contact area but also variations in the amount of fracture filling are likely to be part of the explanation for the scattered data. The influence of fracture filling for Äspö HRL and Laxemar data is assumed to be limited. The reasons for this are that data describe deformation zones/fractures with radial flow (see Section 3.2.2). Further, the hydraulic interference tests identify the fracture(s) along the tested borehole that are most transmissive, consequently, fractures with a large amount of fracture filling will not be identified. A possible explanation for the variation in storage coefficient (from 0.1**S* to 10**S*) could be that different types of fractures are identified. The number of contact points (areas) or the distance between them seems to be an important parameter both concerning the stiffness and the fluid flow.

When describing the detailed geometry of a fracture, interlocked fractures are expected to have a small aperture and the more a fracture slides, the less important the contact surfaces between the two discontinuity planes become and the lower the normal stiffness. In addition, the tortuosity is likely to become low and roughness small compared to the aperture. As an example, a higher stiffness is obtained for the bedding planes than for the faults at the Coaraze site. At this site /Guglielmi et al. 2008b/ also comment that fractures that are almost parallel to the topographic slope direction and dip are in general widely open. The average normal stiffness for faults is 19 GPa/m and for bedding planes 115 GPa/m. The corresponding hydraulic apertures are 280 µm for the faults and 60 µm for the bedding planes. Also for data from /Martin et al. 1990/, the lowest stiffness is found for fractures in the sheared fracture zone.

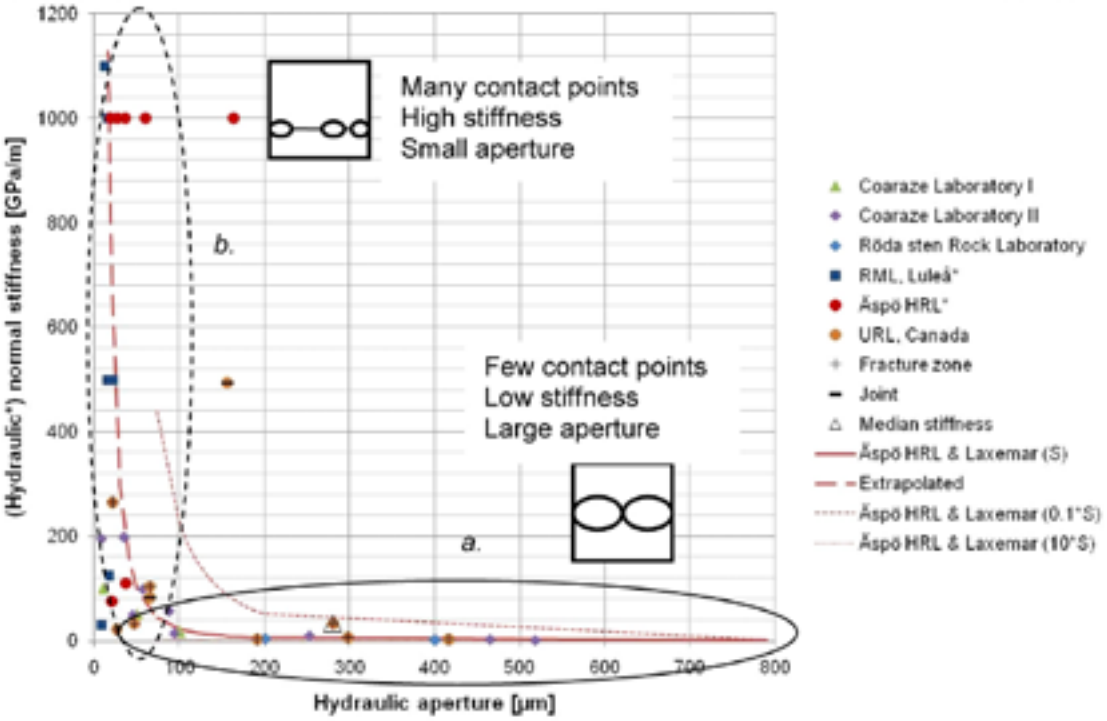

Figure 4-2. *Compilation of (equivalent) hydraulic aperture and normal stiffness (or hydraulic normal stiffness, identified by *). The symbols: +; – and; unfilled triangle are related to URL, Canada data, see section 3.2.1. Coaraze Laboratory I and II originate from the same site but two different papers, see Section 3.1.3.*

The general appearance of Figure 4-2 is in agreement with the results presented in /Guglielmi et al. 2008b/: larger apertures – low stiffness and small apertures – higher stiffness. One interesting reflection concerning the relationship describing Äspö HRL and Laxemar data (Equation 3-3) is that it can be rewritten into the following expression:

$$k_n = \rho_f g \left(\frac{1}{0.0109 \cdot \left(\frac{\rho_f g b_h^{\,3}}{12\mu} \right)^{0.71}} \right) = \frac{C}{b^{3 \cdot 0.71}} = \frac{C}{b^{2.13}} = Cx^{-2.13} \qquad (4\text{-}1)$$

This is in agreement with Equation 2-9 suggested by /Guglielmi et al. 2008b/ that could also be rewritten in the shape of a power-law function:

$$k_n = \frac{1}{a\left(1 - \frac{b}{a} b_h\right)^2} = \frac{k_{n\max}}{\left(1 - \frac{b_h}{b_{h\min}}\right)^2} = Dx^{-2} \qquad (4\text{-}2)$$

C and *D* are constants and both equations indicate that a power-law function could be used to describe the relationship between hydraulic aperture and normal stiffness.

As commented by /Rutqvist and Stephansson 2003/, results from field tests may show a general decrease in permeability with depth (the most pronounced in the upper 100 - 300 meters of the bedrock). However, due to a very large spatial variation in permeability this depth dependency can be difficult to identify. Two extremes are identified, either there are: no or completely mineral cemented or isolated fractures; or there is at least one highly conductive and well connected fracture. The latter

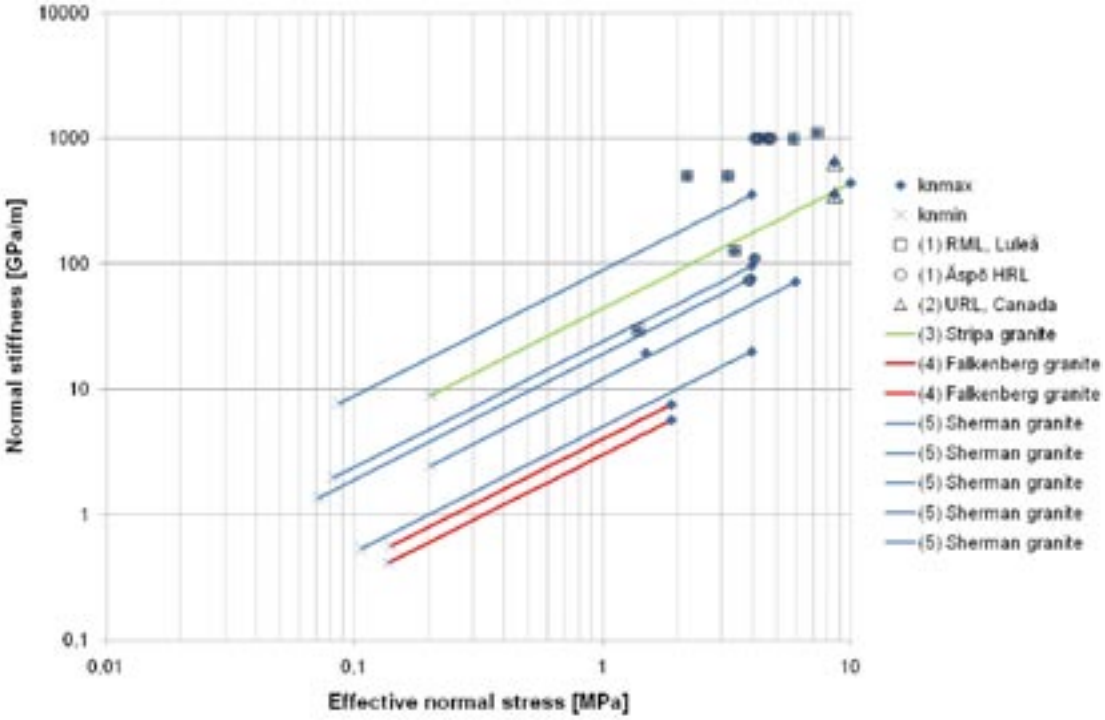

Figure 4-3. *Effective normal stress and estimated normal stiffness, from k_{nmin} to k_{nmax}, using: Equation 11; the intervals of effective normal stress, $\sigma'_{n\,min}$ and $\sigma'_{n\,max}$ and; the stiffness characteristics from /Zangerl et al. 2008/. The references: (1) /Rutqvist et al. 1998/; (2) /Martin et al. 1990/; (3) /Makurat et al. 1990/; (4) /Jung 1989/; and (5) /Pratt et al. 1977/, are included in /Zangerl et al. 2008/.*

can be "locked open" by hard mineral filling or by large shear dislocation. This may occur both in fractures and in fault zones. At greater depth fractures are closed to a residual permeability value. This value is high for locked open fractures. A combination of a large aperture and a high stiffness could be the case for a fracture that is "locked open". According to /Rutqvist and Stephansson 2003/ the bulk permeability at these depths cannot be expected to be especially stress sensitive. Considering the small apertures at high effective stress, hydromechanical experiments on drill cores show that residual void- and hydraulic apertures exist even at very high compressive stress since rock fractures in granite do not close completely /Rutqvist et al. 1998/. Beside deformation, changes in hydraulic aperture can be a result of mineralization, see e.g. /Tullborg et al. 2008/, consequently a change in aperture is not necessarily caused by a change in stress.

None of the field experiments presented in Table 3-1 is found close to a tunnel. For /Alm 1999/ boreholes are drilled in the tunnel floor but according to Kirsch equations /Hoek and Brown 1982/, the fracture should be unaffected by secondary stresses resulting from the tunnel. However, /Alm 1999/ comment that due to the complex geometry of tunnels and caverns, the stress situation is somewhat uncertain. Further, as mentioned by /Gale 1990/ the relationship between fracture orientation and principal stress direction may determine the relative contribution of a fracture set to the rock mass permeability. That a situation with change in stress and permeability may occur close to a tunnel due to redistribution of stresses is commented in e.g. /Hökmark et al. 2006/ and /Rutqvist and Tsang 2008/. Observations related to deformation in the vicinity of tunnels are found within the area of tunnel grouting. One example occurred during a grouting experiment at Äspö HRL at 450 m depth where a possible fracture deformation was identified by the sound of the rock when closing the packer of a borehole /Funehag 2008/. In this case, the borehole intersected a larger conductive fracture. Indication of hydromechanical effects due to grouting has also been identified at e.g. Botniabanan in Sweden /Gothäll and Stille 2008/, where a change in grouting pressure during grouting resulted in a larger than expected increase in grout flow. In addition, the importance of the in situ stress is discussed by /Beitnes 2005/ in a study of the post-excavation grouting at Romeriksporten, Norway. Data obtained from this area could be a valuable source of information for further development concerning hydromechanical coupling. Some initial ideas are presented in /Fransson et al. 2007/.

4.2 Equivalent mechanical properties: rock and fractures

The following includes a suggestion of how to estimate equivalent mechanical properties for rock and fractures and includes field data as a mean to show that this is a reasonable approach. If testing individual fractures or deformation zones the hypothesis is that the individual (only) fracture or the (open) fracture with the lowest stiffness within the deformation zone will be of greatest importance for the result. This is reasonable if assuming that:

- A deformation zone consists of a large number of fractures (high fracture frequency).
- These fractures have different transmissivities and hydraulic apertures. Only a few fractures have a large aperture and several have a small aperture (see Figures 4-4 and 4-5). This has been described by e.g. /Fransson 2002, Gustafson and Fransson 2005/, among others. In /Gustafson and Fransson 2005/, the largest aperture, b_{hr}, is given the lowest rank, r.
- There is a coupling between hydraulic aperture and stiffness, k_n, according to Figures 4-1 and 4-2, where the large aperture fractures tend to have low fracture normal stiffness (largest aperture, b_{hr}, has the lowest normal stiffness, k_{nr}).
- The compressibility of a fracture or the fracture normal compliance (e.g. /Zimmerman 2008/ is the inverse of the fracture stiffness. According to e.g. /Guglielmi et al. 2008a/ equivalent properties for rock and fractures can be estimated using:

$$\frac{1}{E_{eq}} = \frac{1}{E_{matrix}} + \frac{1}{nk_n} \tag{4-3}$$

  where E_{eq} is the compliant Young's modulus, E_{matrix} is the intact rock modulus, k_n is the normal stiffness and n is the fracture spacing per meter of faults or bedding planes.

Based on the above, Equation 4-3 could also be written:

$$\frac{1}{E_{eq}} = \frac{1}{E_{matrix}} + \sum \frac{1}{k_{nr}} \tag{4-4}$$

As an example, a borehole intersecting one large and several small aperture fractures (b_{h1}: large, b_{h2}–b_{h5}: small, k_{n1}: 2 GPa/m: k_{n2}–k_{n5}: 200 GPa/m or less, E_{matrix}: 50 GPa), the stiffness of the large aperture fracture would be most important for the result. In this case, it is important to remember that a combination of a large aperture and a high stiffness could be the case for a fracture that is "locked open". For a small aperture fracture with few points of contact a low stiffness could be expected. This could be in agreement with the comments and results from e.g. /Barton et al. 1985/ where smooth joints in weak rocks are likely to close most readily under normal stress, low shear strength and weak coupling between shearing and conductivity. Rough joints in strong rocks are expected to close least under normal stress, have high shear strength and strong coupling between shearing and conductivity.

4.2.1 Fractures: Transmissivity distributions, fracture frequency and depth

Below are presented field data and references that are in line with what is presented above. Figure 4-4 and Figure 4-5 present estimated individual fracture transmissivity distributions for boreholes at Forsmark /SKB 2005a/, Laxemar /SKB 2005b/ and Olkiluoto, Finland, see e.g. /Fransson 2002, Gustafson and Fransson 2005/. Further, a Pareto distribution was fit to the data, see /Gustafson and Fransson 2005/.

Figure 4-4 presents individual fracture transmissivity distributions estimated for three different depths (levels) for two boreholes at Forsmark. The two figures confirm that most fractures will have a small transmissivity or aperture (large probability that the aperture is smaller than e.g. 100 μm, dashed line) and few fractures will have a large transmissivity (aperture), particularly the deepest section.

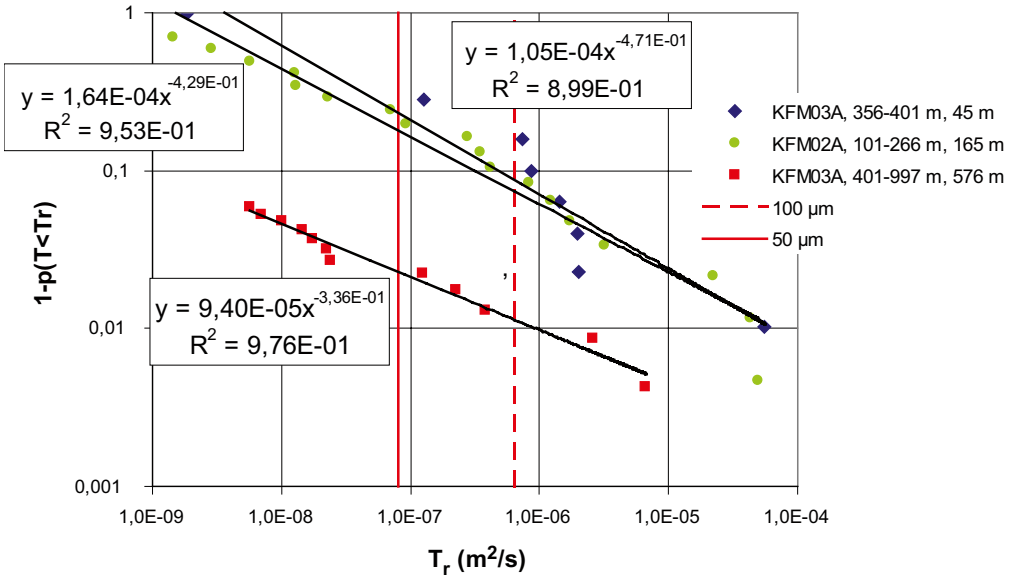

Figure 4-4. *Transmissivity distributions for individual fractures (and fitted Pareto distributions) estimated for three different depths (levels) from two different boreholes at Forsmark. Includes two red lines representing transmissivities for fractures with an aperture of 50 and 100 µm.*

Relating these data to the hydraulic apertures in Figure 4-2, borehole KFM03A, (401–997 m) is expected to have the highest effective stress (large depth) and the smallest hydraulic apertures (mainly included in the group limited by the dashed line corresponding to an aperture of 100 µm, Figure 4-4). Based on the results from this analysis, the probability that the transmissivity of fractures is smaller than $1 \cdot 10^{-6}$ m^2/s is 0.99 (Figure 4-4). Further, KFM02A (101–266 m) is assumed to represent a rock domain and KFM03A (356–401 m) a zone. According to Figure 4-4, they have similar distributions but the fracture frequency differs. These data could be part of both groups identified in Figure 4-2 and the probability that the transmissivity of fractures is smaller than $1 \cdot 10^{-6}$ m^2/s is approximately 0.9. Consequently, a higher percentage of the fractures is likely to have large apertures. The effective stress is expected to be lower due to the smaller depth and the intersection of a zone. Figure 4-5 presents another example of transmissivity distributions (and fitted Pareto distributions) estimated for three boreholes at Forsmark, Laxemar and Olkiluoto, Finland.

4.2.2 Behaviour of deformation zones

According to Figures 4-1 and 4-2, large aperture fractures tend to have the lowest stiffness and would therefore deform more easily. Above is suggested that this could be the case both when a fracture is part of a deformation zone and when it is not. Results from Äspö /Rutqvist et al. 1998/ present high effective stresses and small apertures (increased joint closure). Here, few open fractures dominated the inflow but they were still part of the most conductive zones intersecting the tested borehole (KLX02). For /Martin et al. 1990/ some tests within the deformation zone have a low effective stress and larger apertures, but here as well, some sections present higher effective stress, smaller apertures and higher stiffness. One example is a section with an effective stress of 20 MPa, an aperture of 20 µm and a stiffness of 270 GPa/m. Data describe a deformation zone but the behavior could be linked to the individual fractures and the situation of stress. Data based on the results from /Rhén et al. 2008/ are also in agreement with the investigations of individual fractures even though the data originate from investigations of deformation zones.

/Seront et al. 1998/ investigating a normal fault suggest that fluid flow and changes in fluid storage are concentrated in the damage zone. A damage zone containing arrays of mesoscopic fractures. Further, /Evans et al. 2005/ comment that the creation and enhancement of permeability was limited to the hydrothermally altered sections at the intersection of cataclastic shear zones. Zones where almost all the naturally permeable fractures were located. Major structures with a strongly developed alteration

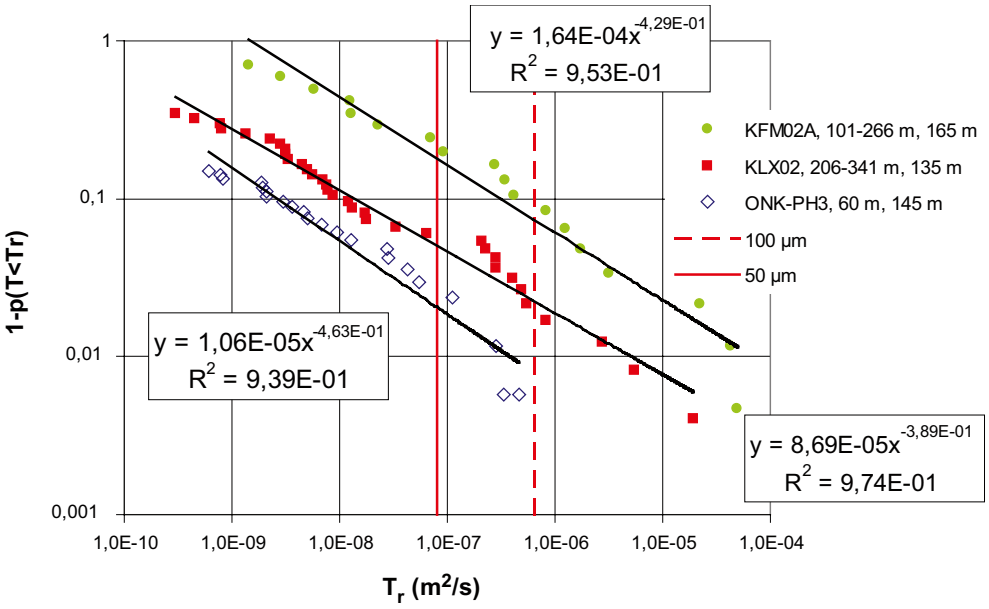

Figure 4-5. *Transmissivity distributions for individual fractures (and fitted Pareto distributions) estimated for three boreholes at Forsmark, Laxemar and Olkiluoto, Finland. Includes two red lines representing transmissivities for fractures with an aperture of 50 and 100 µm.*

did appear to be less susceptible to transmissivity enhancement through shear than lesser structures. According to the authors the mechanisms are uncertain but it could be due to e.g. the effects of alteration resulting in smoother fracture surfaces. For /Martin et al. 1990/ boreholes were tested in sections and here as well the cataclastic zone was important since a significant decrease in normal stiffness was found when the measurements approached this zone. For these data (see Figure 4-1 and Figure 4-2), a better agreement for large aperture data would be found if using the lowest stiffness instead of the median stiffness for the URL data point (triangle). In general the references on fault zones presented here agree on the description presented by /Chester and Logan 1986/ suggesting a model with three mechanical units including: the undeformed host rock; a damaged zone; and a gouge layer. Discussing the hydrogeology of weathered granites from a more general perspective based on permeability data from e.g. Hong Kong and Singapore, /Hartwell 2007/ describe the weathering of granite from fresh intact rock to residual soil (referred to as Grade I to Grade VI). The author comments that as weathering progresses in Grade III and IV material (weak rock, can be broken by hand), the fissure flow will still dominate even though intergranular permeability and porosity will start to develop. The author concludes that the highest permeabilites are found at the "rockhead" interface (more fractures and an absence of clay infilling, Grade IV and V materials).

According to the above, the individual fracture transmissivity and hydraulic aperture (including variations described by the fracture being interlocked to mismatched) seem to be key parameters. Taking the reasoning one step further and comparing: (1) the deformation of two parallel fractures, one with large and one with small aperture and; (2) a deformation zone, including a large aperture fracture and a section of broken and weathered rock. In both cases the references suggest that the large aperture fracture is more likely to deform. One idea could be to link this to the specific surface area of the material, e.g. /Carman 1937/ or the relation between the volume available to flow and the area of the geological material, where a viscous drag along the grain walls will appear. For the broken rock (and the small aperture fracture) the flow resistance will be large resulting in a faster decrease in pressure (larger gradient) close to a tested borehole and a smaller radius of influence compared to the large aperture fracture. Consequently the increase in fluid pressure for the large aperture fracture would be larger and the fracture would be more likely to open up and increase the stress over the adjacent features. This is in agreement with modeling performed by /Guglielmi et al. 2008b/ showing that in case of parallel fractures, poroelastic opening of a tested fracture induces a poroelastic closing of the surrounding parallel fractures.

4.3 Impact of shear stress and displacement on transmissivity

Detailed field data considering shear deformation and transmissivity were not found but relations between shear stress and deformation are described by e.g. /Bandis et al. 1983, Barton et al. 1985, Olsson and Barton 2001/. Both normal and shear stresses influence the deformation and /Guglielmi et al. 2008b/ describe the situation for a fracture where the opposing joint walls are pressed together under a positive effective normal stress. In addition, the shear stress acts parallel to the fracture plane and perpendicular to the effective normal stress that resists a sliding motion. Reducing the effective normal stress leads to a normal opening and reduced shear strength. During fracture shear movements the aperture will change due to dilation. In this case the asperities can be sheared through or overridden. Further, /Gentier et al. 2000/ conclude that the mechanical behavior of fractures under shear stress is strongly related to the geometry of the fracture surfaces. Direction of shear is important and related parameters are peak shear stress, residual shear stress, dilatancy and displacement at peak shear stress, and shear stiffness. /Evans et al. 1999/ comment that for fractures that are verging on shear failure at the prevailing stress conditions, shear displacement can occur for small pressure increases. In addition, for permanent increases in the transmissivity of flow paths the authors suggest that shear displacement is the most credible mechanism. The theoretical difficulties are highlighted in /Koyama et al. 2008/ commenting that the impact of the surface roughness of rock fractures is still an unresolved issue. The paper investigates the effects of shear displacements on the magnitudes and anisotropy of the fluid flow velocity field.

Investigations and results on shear and transmissivity are found in /Talbot and Sirat 2001/ investigating the occurrence of wet fractures in the tunnel of the Äspö Hard Rock Laboratory. Above 240 m depth, most wet fractures are subhorizontal (stress regime prone to thrusting). Below this depth they are subvertical with NW trends (stress regime prone to wrench faulting). The authors comment that the most active groundwater flow pathways tend to be faults that have a favourable orientation for slip or dilation in the ambient stress field. In /Guglielmi et al. 2008a/ analyses for a field site in carbonate rock, the Coaraze Laboratory site, result in an estimated shear stiffness of one-tenth of the normal stiffness but field measurements were not made. The authors express an urgent need to develop in situ measurements of both normal and shear displacements. So even though modeling efforts in general, e.g. /Walsh et al. 2008/, are useful and describe the problem, it is important to improve investigation methods and combine field testing and analysis (modelling) to increase the understanding and the ability to investigate the behaviour in situ.

5 Summary and conclusions

The importance of the topic of this literature survey is underlined by the comment in the review paper of /Rutqvist and Stephansson 2003/ saying that a key parameter in a coupled hydromechanical analysis is a good estimate of the relationship between stress and permeability. Considering the line of research, the following steps in the development can be identified:

1. Investigations of the fundamentals of rock joint deformation. Strength, deformation and conductivity coupling of rock joints. Identification and description of mechanisms in the laboratory. /Bandis et al. 1983, Barton et al. 1985, Evans et al. 1992, Goodman 1974, Witherspoon et al. 1980/.
2. Coupling of stress-flow properties of rock joints from hydraulic field testing. Identification and description of mechanisms in the field. Individual fractures, deformation zones. /Rutqvist 1995, Alm 1999, Martin et al. 1990, Talbot and Sirat 2001/.
3. In situ investigations. Identification and description of mechanisms in the field including investigation and description of system of fractures, different types of fractures (interlocked/mated or mismatched/unmated) and how this is coupled to the hydromechanical behavior. /Cappa et al. 2006, Guglielmi et al. 2008b, Zangerl et al. 2008/.

5.1 Impact of normal stress change and deformation on transmissivity

Data originating from investigations of both fractures and deformation zones have been compiled. To motivate that this is a reasonable approach, the report also includes a suggestion on how to estimate equivalent mechanical properties for rock and fractures. The hypothesis is that if individual fractures or deformation zones are subjected to a change in stress, the individual (only) fracture or the (open) fracture with the lowest stiffness within the deformation zone will be of greatest importance for the behavior.

Figure 4-1 (log-log plot) and Figure 4-2 (lin-lin plot) compile data from most of the references presented in Table 3-1. The figures include hydraulic aperture (equivalent) and hydraulic normal stiffness from /Rutqvist et al. 1998, Alm 1999, Cappa et al. 2006, Guglielmi et al. 2008b, Martin et al. 1990, Rhén et al. 2008/. The largest apertures in general have the lowest stiffness but also the lowest effective normal stress. For data from /Rutqvist et al. 1998/ (RML, Luleå and Äspö HRL) the hydraulic normal stiffness is included in the figures and multiplying this stiffness by the factor f of 0.3 (see Sections 2.2.1 and 3.1.1), would not change the general appearance of the figure to any large extent.

Concerning the figures, the following comments are considered important:

- All data except those from the Coaraze site originate from granitic rock (see Table 3-1). Even so, the data seem to be in good agreement.
- Normal stiffness, k_n, and hydraulic aperture, $b_{h,}$ are correlated, even though data are scattered. For Äspö HRL and Laxemar data, the relation between k_n and b_h (Equations 3-1 to 3-3) based on 0.1*S and 10*S are also included since the storage coefficient, S, for a certain transmissivity, T, are found within this interval. In general, the largest variation is seen for the smallest hydraulic apertures.
- Data from Äspö HRL and Laxemar /Rhén et al. 2008/ estimated from the storage coefficient, S, and transmissivity; T, from hydraulic interference tests seems to agree as well thus giving a relationship between the parameters, normal stiffness, k_n, storage coefficient, S, and hydraulic aperture, b_h for the data. This presents a possibility to estimate k_n and b_h based on storage coefficient, S, and transmissivity, T, from hydraulic interference tests for the investigated area.

Based on the compilation of data and references, the description in Figure 5-1 is suggested.

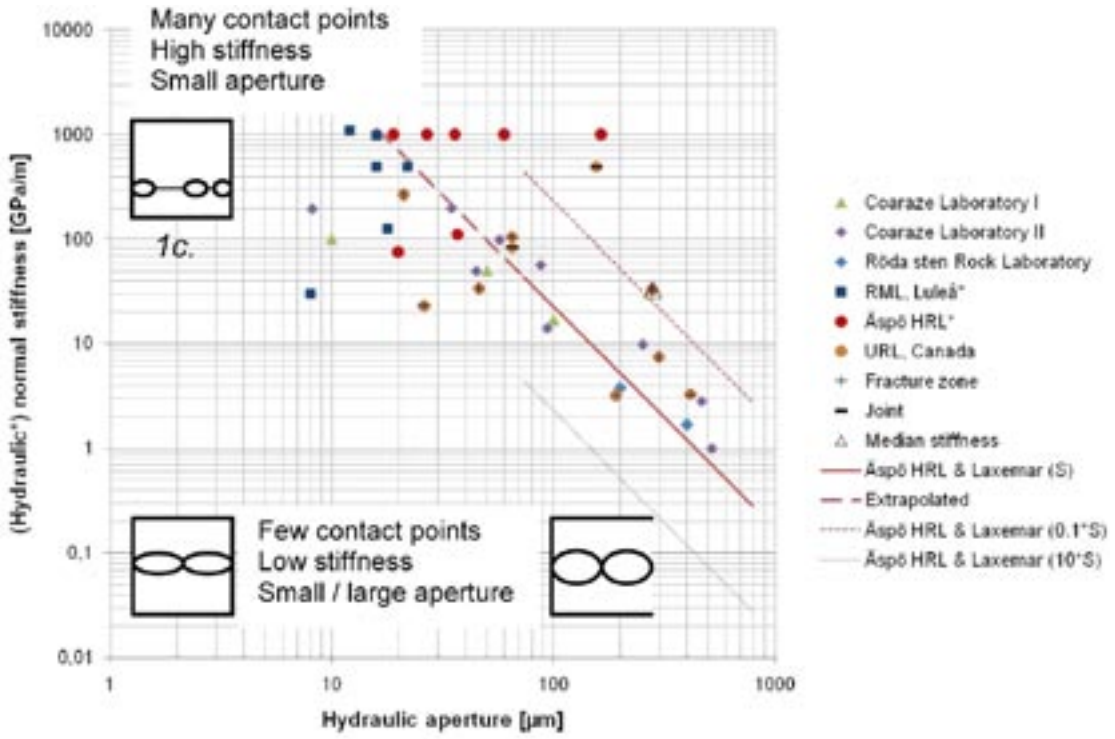

Figure 5-1. *Compilation of (equivalent) hydraulic aperture and normal stiffness (or hydraulic normal stiffness, identified by *). The symbols: +; – and; unfilled triangle are related to URL, Canada data, see section 3.2.1. Three sketches based on Figures 2-1a and 2-1c are included representing: (1a) fracture surfaces brought into contact with a minimum normal load; and (1c) The load and the deformation increases forming additional points of contact. Coaraze Laboratory I and II originate from the same site but two different papers, see Section 3.1.3.*

In the figure, three simplified sketches based on Figure 2-1a and Figure 2-1c are included:

- In the lower right hand corner (1a, large aperture – low stiffness), few contact points, low stiffness and large aperture is expected (low effective stress). A radial flow is more likely compared to fractures represented by data described in the point below (many points of contact more likely to result in 1D, channeled flow). Äspö HRL and Laxemar data are found within the lines represented by 0.1**S* and 10**S*. The influence of fracture filling for Äspö HRL and Laxemar data is assumed to be limited. The reasons for this are that data describe deformation zones/fractures with radial flow (see Section 3.2.2). Further, the hydraulic interference tests identify the fracture(s) along the tested borehole that are most transmissive, consequently, fractures with a large amount of fracture filling will not be identified. A possible explanation for the variation in storage coefficient (from 0.1**S* to 10**S*) could be that different types of fractures are identified. The simplified sketch to the left of sketch 1a, Figure 5-1, having few contact points, low stiffness and a small aperture could be one example.
- In the upper left hand corner (1c, small aperture – high stiffness), many contact points, high stiffness and a small aperture is expected (high effective stress). These data are more scattered than those presented above. Variations in contact area (transferring stresses and influencing the estimate of hydraulic aperture) but also variations in the amount of fracture filling (influencing the estimate of hydraulic aperture) are likely to be part of the explanation for the scattered data. Intersecting one of the channels is likely to result in an overestimated aperture. This could e.g. be the case for the large aperture – high stiffness data from Äspö HRL (red filled circles). If a borehole is intersecting a channel or a part of the fracture were the fracture surfaces are in contact would give different results when estimating the hydraulic aperture.

For a group of smoother fractures e.g. for another type of fracture within the same rock or for another type of rock, one could imagine fractures having fewer points of contact and lower stiffness compared to the solid line (Äspö HRL & Laxemar) included in Figure 5-1.

The compilation of data indicates that a power-law function (see Equations 4-1 and 4-2) could be used to describe the relationship between hydraulic aperture and normal stiffness.

$k_n = Cx^{-2}$

where x is equal to or depending on the hydraulic aperture, b_h, and C is a constant

The general behaviour presented in Figure 5-1 is in line with /Barton et al. 1985/ commenting that smooth joints in weak rocks are likely to close most readily under normal stress (with low shear strength and weak coupling between shearing and conductivity). Further, rough joints in strong rocks are expected to close least under normal stress (and have high shear strength and strong coupling between shearing and conductivity). This is also in agreement with the review paper by /Rutqvist and Stephansson 2003/ that concludes that the permeability of rock masses at shallow depth (low stress) and in areas of low in situ permeability tends to be most sensitive to stress changes. The authors comment that results from field tests may show a general decrease in permeability with depth (the most pronounced in the upper 100–300 meters of the bedrock). However, due to a very large spatial variation in permeability this depth dependency can be difficult to identify. Two extremes are identified, either there are: no or completely mineral cemented or isolated fractures; or there is at least one highly conductive and well connected fracture. Highly permeable fractured rock sections where fractures are "locked open" by hard mineral filling or by large shear dislocation seem to be less sensitive and can be conductive also at great depths. According to /Rutqvist and Stephansson 2003/, the bulk permeability at these depths cannot be expected to be especially stress sensitive. Considering the small apertures at high effective stress, hydromechanical experiments on drill cores show that residual void- and hydraulic aperture exist even at very high compressive stress since rock fractures in granite do not close completely /Rutqvist et al. 1998/. Beside deformation, changes in hydraulic aperture can be a result of mineralization, see e.g. /Tullborg et al. 2008/, consequently a change in aperture is not necessarily caused by a change in stress.

In general the references on fault zones presented here agree on the description presented by /Chester and Logan 1986/ suggesting a model with three mechanical units including: the undeformed host rock; a damaged zone; and a gouge layer. There also seem to be an agreement that a strongly sheared fault core would hinder fluid flow and mainly allowing large flow through the damaged zone.

5.1.1 Equivalent mechanical properties: rock and fractures

If testing individual fractures or deformation zones the hypothesis is that the individual (only) fracture or the (open) fracture with the lowest stiffness within the deformation zone will be of greatest importance for the behaviour. This is reasonable if assuming that there is a coupling between hydraulic aperture and stiffness, k_n, according to Figures 4-1 and 4-2, where the large aperture fractures tend to have low fracture normal stiffness (largest aperture, $b_{hr} = b_{h1}$, has the lowest normal stiffness, $k_{nr} = k_{n1}$). The following expression for estimate of an equivalent Young's modulus is suggested:

$$\frac{1}{E_{eq}} = \frac{1}{E_{matrix}} + \sum \frac{1}{k_{nr}} \tag{5-1}$$

where the stiffness of the large aperture fracture with the lowest stiffness would be most important for the result. If only one individual fracture, this fracture will influence the result in relation to its stiffness. It is important to remember that a combination of a large aperture and a high stiffness could be the case for a fracture that is "locked open". For a small aperture fracture with few points of contact a low stiffness could be expected. Based on this literature survey the above is e.g. indicated by:

- Modeling performed by /Guglielmi et al. 2008b/ showing that in case of parallel fractures, poroelastic opening of a tested fracture induces a poroelastic closing of the surrounding parallel fractures. According to the compilation (Figures 4-1 and 4-2), large aperture fractures tend to have the lowest stiffness and would therefore deform more easily.
- Results from Äspö /Rutqvist et al. 1998/ including higher effective stresses and small apertures (increased joint closure). Few open fractures dominated the inflow but they were still part of the most conductive zones intersecting the tested borehole (KLX02).

- For /Martin et al. 1990/ some tests within the deformation zone have a low effective stress, larger apertures and low stiffness, but here as well, some sections present higher effective stress, smaller apertures and higher stiffness. Data describe a deformation zone but the behavior could be linked to the individual fractures and the situation of stress. One example is that a better agreement for large aperture data would be found if using the lowest stiffness (4.4 GPa/m) instead of the median stiffness for the URL data point (unfilled triangle, Figures 4-1, 4-2 and 5-1).
- Data based on the results from /Rhén et al. 2008/ describes the behavior of deformation zones. These data seem to be in agreement with the investigations of individual fractures.

Observations related to deformation in the vicinity of tunnels are found within the area of tunnel grouting. Data obtained from this area could be a valuable source of information for further development concerning hydromechanical coupling. Some initial ideas are presented in /Fransson et al. 2007/.

5.2 Impact of shear stress and displacement on transmissivity

No detailed field data was found on the impact of shear stress and displacement on transmissivity. This is in line with the comment by /Guglielmi et al. 2008b/ where the authors express an urgent need to develop *in situ* measurements of both normal and shear displacements.

/Evans et al. 1999/ comment that for fractures that are verging on shear failure at the prevailing stress conditions, shear displacement can occur for small pressure increases. In addition, for permanent increases in the transmissivity of flow paths the authors suggest that shear displacement is the most credible mechanism.

Based on laboratory experiments, relations between shear stress and deformation are described by e.g. /Bandis et al. 1983, Barton et al. 1985, Olsson and Barton 2001/. The impact of shear stress and displacement on transmissivity for different normal load conditions is reflected in Equation 2-15 where the parameter M, referred to as a damage coefficient is given values of 1 or 2 for shearing under low or high normal stress respectively. A smaller aperture and transmissivity is the result for shearing under high normal stress.

In /Guglielmi et al. 2008b/ analyses for a field site in carbonate rock, the Coaraze Laboratory site, results in estimated shear stiffness of one-tenth of the normal stiffness but field measurements were not made. Comments on shear and transmissivity are found in /Talbot and Sirat 2001/ investigating the occurrence of wet fractures in the tunnel of the Äspö Hard Rock Laboratory. The most active groundwater flow pathways tend to be faults that have a favourable orientation for slip or dilation in the ambient stress field. So even though modeling efforts, e.g. /Walsh et al. 2008/, are useful and describe the problem. It is important to improve investigation methods and combine field testing and analysis (modelling) to increase the understanding and the ability to investigate the behaviour *in situ*.

5.3 Concluding remark

To conclude, impact of normal stress change and deformation on transmissivity could be described based on data from *in situ* investigations. The results shown in this compilation present a possibility to estimate normal stiffness, k_n and hydraulic aperture, b_h based on storage coefficient, S, and transmissivity, T, from hydraulic interference tests performed in the area of interest. Concerning the impact of shear stress and displacement on transmissivity, no detailed field data was found. This is in line with the comment by /Guglielmi et al. 2008b/ where the authors express an urgent need to develop *in situ* measurements of both normal and shear displacements. Further research within the area of hydromechanical coupling where geology, hydrogeology and geomechanics meet is likely to increase the understanding of all these areas.

References

Alm P, 1999. Hydro-mechanical behaviour of a pressurized single fracture: an in situ experiment. Ph.D. thesis, Chalmers University of Technology, Göteborg.

Andersson J, Christiansson R, Hudson J, 2002. Site investigations Strategy for rock mechanics site descriptive model. SKB TR-02-01, Svensk Kärnbränslehantering AB.

Bandis S, Lumsden AC, Barton N R, 1983. Fundamentals of rock joint deformation. International Journal of Rock Mechanics Mining Sciences & Geomech Abstr., Vol. 20, No. 6, pp 249–268.

Barton N, Bandis S, Bakhtar K, 1985. Strength, deformation and conductivity coupling of rock joints. International Journal of Rock Mechanics Mining Sciences & Geomech Abstr., Vol. 22, No. 3, pp 121–140.

Beitnes A, 2005. Lessons to be learned from Romeriksporten. Tunnels and Tunnelling International, Vol. 37, No. 6, Juni, pp. 36–38.

Bense V F, Van den Berg E H, Van Balen R T, 2003. Deformation mechanisms and hydraulic properties of fault zones in unconsolidated sediments; the Roer Valley Rift System, The Netherlands. Hydrogeology Journal, Vol. 11, No. 3, pp 319–332.

Cappa F, Guglielmi Y, Rutqvist J, Tsang C-F, Thorval A, 2006. Hydromechanical modeling of pulse tests that measure fluid pressure and fracture normal displacement at the Coaraze Laboratory site, France. International Journal of Rock Mechanics and Mining Sciences, Vol. 43, No. 7, pp 1062–1082.

Carman P C, 1937. Fluid flow through granular beds. Trans. Instn. chem. Engrs, 15:150–166.

Chester F M, Logan J M, 1986. Implications for mechanical properties of brittle faults from observations of the Punchbowl Fault Zone, California. Pure and Applied Geophysics, Vol. 124, Nos. 1/2, pp.79–106.

Doe T, Geier J, 1990. Interpretations of fracture system geometry using well test data. SKB Stripa Project TR 91-03, Svensk Kärnbränslehantering AB.

Evans KF, Kohl T, Hopkirk R J, Rybach L, 1992. Modeling of energy production from hot dry rock systems. Proj Rep Eidgenösische Technische Hochschule (ETH), Zurich, Switzerland.

Evans J P, Forster C B, Goddard J V, 1997. Permeability of fault-related rocks, and implications for hydraulic structure of fault zones. Journal of Structural Geology, Vol. 19, No. 11, pp. 1393–1404.

Evans K F, Cornet F H, Hashida T, Hayashi K, Ito T, Matsuki K, Wallroth T, 1999. Stress and rock mechanics issues of relevance to HDR/HWR engineered geothermal systems: review of developments during the past 15 years. Geothermics, Vol. 28, pp 455–474.

Evans K F, Genter A, Sausse J, 2005. Permeability creation and damage due to massive fluid injections into granite at 3.5 km at Soultz: 1. Borehole observations. Journal of geophysical research, Vol 110, pp 1–19.

Fransson Å, 2002. Nonparametric method for transmissivity distributions along boreholes. Ground Water, Vol. 40, No. 2, pp. 201–204.

Fransson Å, Tsang C-F, Rutqvist J, Gustafson G, 2007. A new parameter to assess hydromechanical effect in single-hole hydraulic testing and grouting. Int J Rock Mech Min Sci, Vol. 44, No. 7, pp 1011–1021.

Funehag J, 2008. Injektering av TASS-tunneln Delresultat t o m september 2008. SKB R-08-123, Svensk Kärnbränslehantering AB.

Gale J, 1990. Hydraulic behavior of rock joints. Rock joints (Barton & Stephansson, eds) . Balkema, Rotterdam, Netherlands.

Gentier S, Riss J, Archambault G, Flamand R, Hopkins D, 2000. Influence of fracture geometry on shear behavior. International Journal of Rock Mechanics and Mining Sciences, Vol. 37, No. 1-2, pp 161–174.

Goodman R E, 1974. The mechanical properties of joints. Proceedings of the 3rd Int. Congr. International Society of Rock Mechanics, Denver, Colorado. National Academy of Sciences, Washington, DC, I, 127–140.

Gothäll R, Stille H, 2008. Fracture dilation during grouting, Tunnel. Underg. Space Technol., doi:10.1016/j.tust.2008.05.004.

Gothäll R, 2009. Behaviour of rock fractures under grout pressure loadings Basic mechanisms and special cases. Ph.D. thesis, Royal Institute of Technology, Stockholm.

Guglielmi Y, Cappa F, Rutqvist J, Tsang C-F, Thoraval A, 2008a. Mesoscale characterization of coupled hydromechanical behavior of a fractured-porous slope in response to free water-surface movement. International Journal of Rock Mechanics and Mining Sciences, doi: 10.1016/j.ijrmms.2007.09.010. Vol. 45, No. 6, pp 862–878.

Guglielmi Y, Cappa F, Virieux J, Rutqvist J, Tsang C-F, Thoraval A, 2008b. A new in situ approach for hydromechanical characterization of mesoscale fractures: the High-Pulse Poroelasticity Protocol (HPPP). 42nd US Rock Mechanics Symposium and 2nd U.S.-Canada Rock Mechanics Symposium, June 29 – July 2, San Francisco, California.

Gustafson G, Fransson Å, 2005. The Use of the Pareto Distribution for Fracture Transmissivity Assessment. Hydrogeol J, Vol. 14, No. 1-2, pp. 307–313.

Hakami E, 1995. Aperture distribution of rock fractures. PhD thesis, Royal Institute of Technology, Stockholm.

Hartwell D J, 2007. The hydrogeology of weathered granites. Proceedings of the 10th Australia New Zealand Conference on Geomechanics, Brisbane, Australia.

Hoek E, Brown E T, 1982. Underground excavation in rock. E & FN Spon, London.

Hökmark H, Fälth B, Wallroth T, 2006. T-H-M couplings in rock. Overview of results of importance to the SR-Can safety assessment. SKB R-06-88, Svensk Kärnbränslehantering AB.

Jung R, 1989. Hydraulic in situ investigations of an artificial fracture in the Falkenberg Granite. International Journal of Rock Mechanics and Mining Sciences, Vol. 26, No. 3/4, pp 301–308.

Kohl T, Evans K F, Hopkirk R J, Rybach L, 1995. Coupled hydraulic, thermal and mechanical considerations for the simulation of hot dry rock reservoirs. Geothermics, Vol. 24, No. 3, pp. 345–359.

Koyama T, Neretnieks I, Jing L, 2008. A numerical study on differences in using Navier-Stokes and Reynolds equations for modeling the fluid flow and particle transport in single rock fractures with shear. International Journal of Rock Mechanics and Mining Sciences, Vol. 45, No. 7, pp 1082–1101.

Makurat A, Barton N, Tunbridge L, Vik G, 1990. Rock joints (Barton & Stephansson, eds). The measurement of the mechanical and hydraulic properties of rock joints at different scales in the Stripa project. Balkema, Rotterdam, Netherlands.

Martin C D, Davison C C, Kozak E T, 1990. Rock joints (Barton & Stephansson, eds). Characterizing normal stiffness and hydraulic conductivity of a major shear zone in granite. Balkema, Rotterdam, Netherlands.

Munier R, Stanfors R, Milnes A G, Hermanson J, Triumf C-A, 2003. Geological site descriptive model A strategy for the model development during site investigations. SKB R-03-07, Svensk Kärnbränslehantering AB.

Olsson R, 1998. Mechanical and hydromechanical behaviour of hard rock joints: A laboratory study. Ph.D. thesis, Chalmers University of Technology, Göteborg.

Olsson R, Barton N, 2001. An improved model for hydromechanical coupling during shearing of rock joints. International Journal of Rock Mechanics and Mining Sciences, Vol. 38, No. 3, pp 317–329.

Pratt H R, Swolfs H S, Brace W F, Black A D, Handin J W, 1977. Elastic and transport properties of an in situ jointed granite. International Journal of Rock Mechanics and Mining Sciences, Vol. 14, No. 1, pp 34–45.

Rhén I, Follin S, Hermanson J, 2003. Hydrogeological site descriptive model – a strategy for its development during site investigations. SKB R-03-08, Svensk Kärnbränslehantering AB.

Rhén I, Forsmark T, Hartley L, Jackson P, Roberts D, Swan D, Gylling B, 2008. Hydrogeological conceptualisation and parameterisation, Site descriptive modelling SDM–Site Laxemar, SKB R-08-78, Svensk Kärnbränslehantering AB.

Rutqvist J, 1995. Coupled stress-flow properties of rock joints from hydraulic field testing. Ph.D. thesis, Royal Institute of Technology, Stockholm.

Rutqvist J, Noorishad J, Tsang C-F, Stephansson O, 1998. Determination of fracture storativity in hard rocks using high-pressure injection testing. Water Resources Research, Vol. 34, No. 10, pp. 2551–2560.

Rutqvist J, Stephansson O, 2003. The role of hydromechanical coupling in fractured rock engineering. Hydrogeol. J.,11,7–40.

Rutqvist J, Tsang C-F, 2008. Review of SKB´s work on coupled THM processes within SR-Can. External review contribution in support of SKI´s and SSI´s review of SR-Can. SKI Report 2008:08, Swedish Nuclear Power Inspectorate, Stockholm, Sweden.

Seront B, Wong T-F, Caine J S, Forster C B, Bruhn R L, Fredrich J T, 1998. Laboratory characterization of hydromechanical properties of a seismogenic normal fault system. Journal of structural geology, Vol.20, No. 7, pp. 865–881.

SKB, 2005a. Preliminary site description. Forsmark area – version 1.2. SKB R-05-18, Svensk Kärnbränslehantering AB.

SKB, 2005b. Preliminary site description. Simpevarp subarea – version 1.2. SKB R-05-08, Svensk Kärnbränslehantering AB.

Talbot C J, Sirat M, 2001. Stress control of hydraulic conductivity in fracture-saturated Swedish bedrock. Engineering geology, Vol. 61, No. 2-3, pp. 145–153.

Tullborg E-L, Drake H, Sandström B, 2008. Palaeohydrogeology: A methodology based on fracture mineral studies. Applied Geochemistry, Vol. 23, No. 7, pp. 1881–1897.

Walsh R, McDermott C, Kolditz O, 2008. Numerical modeling of stress-permeability coupling in rough fractures. Hydrogeology Journal, Vol. 16, No. 4, pp.613–627.

Wibberley A J, Shimamoto T, 2003. Internal structure and permeability of major strike-slip fault zones: the Median Tectonic Line in Mie Prefecture, Southwest Japan. Journal of structural geology, Vol. 25, No. 1, pp. 59–78.

Witherspoon P A, Wang J S Y, Iwai K, Gale J E, 1980. Validity of the cubic law for fluid flow in a deformable fracture. Water Resources Research, Vol. 16, No. 6, pp. 1016–1024.

Zangerl C, Evans K F, Eberhardt E, Loew S, 2008. Normal stiffness of fractures in granitic rock: A compilation of laboratory and in situ experiments. International Journal of Rock Mechanics and Mining Sciences, Vol. 45, No. 8, pp. 1500–1507.

Zhang S, Tullis E T, Scruggs V J, 1999. Permeability anisotropy and pressure dependency of permeability in experimentally sheared gouge materials. Journal of structural geology, Vol. 21, No. 7, pp. 795–806.

Zimmerman R W, 2008. A simple model for coupling between the normal stiffness and the hydraulic transmissivity of a fracture. 42nd US Rock Mechanics Symposium and 2nd U.S.-Canada Rock Mechanics Symposium, June 29 – July 2, San Francisco, California.